JPET Fast Forward. Published on May 28, 2010 as DOI: 10.1124/jpet.110.167528

JPET #167528

$P2Y_2$ receptor-$G_{q/11}$ signaling at lipid rafts is required for UTP-induced cell migration in NG 108-15 cells

Koji Ando, Yutaro Obara, Jun Sugama, Atsushi Kotani, Nobuyuki Koike, Satoko Ohkubo and Norimichi Nakahata

Department of Cellular Signaling, Graduate School of Pharmaceutical Sciences, Tohoku University, Aoba 6-3, Aramaki, Aoba-ku, Sendai 980-8578, Japan (K.A., Y.O., J.S., A.K., N.K., S.O., N.N.) and Division of Pharmacology, National Institute of Health Sciences, Kamiyoga 1-18-1, Setagaya-ku, Tokyo 158-8501, Japan (S.O.)

JPET Fast Forward. Published on May 28, 2010 as DOI: 10.1124/jpet.110.167528
This article has not been copyedited and formatted. The final version may differ from this version.

a) Running Title; Role of lipid rafts in $P2Y_2$ receptor-$G_{q/11}$ signaling.

b) Correspondence: Norimichi Nakahata, Ph.D.
Department of Cellular Signaling
Graduate School of Pharmaceutical Sciences
Tohoku University
Aoba 6-3, Aramaki, Aoba-ku, Sendai 980-8578
Japan
(TEL) +81-22-795-6809
(FAX) +81-22-795-3847
(Email) nakahata@mail.pharm.tohoku.ac.jp

c) Text: 41 pages.
Number of Figures: 8
Number of tables: 0
Number of References: 40
Abstract: 228 words
Introduction: 677 words
Discussion: 1195 words

d) Abbreviations

AC, adenylyl cyclase; ALP, alkaline phosphatase; ATP; adenosine 5'-triphosphate; CD, methyl-β-cyclodextrin; DMEM, Dulbecco's modified Eagle's medium; DRM, detergent-resistant membrane; GPCR, G protein-coupled receptor; GPI; glycosylphosphatidylinositol; HEPES; 2-[4-(2-hydroxyl)-1-piperazinyl] ethanesulfonic acid; HRP, horse radish peroxidase; LPA, lysophosphatidic acid; PIP_2, phosphatidylinositol-4,5-bisphosphate; PLC, phospholipase C; RGS, regulator of G-protein signaling; UTP; uridine 5'-triphosphate

e) Recommended Section: Cellular and Molecular

JPET Fast Forward. Published on May 28, 2010 as DOI: 10.1124/jpet.110.167528
This article has not been copyedited and formatted. The final version may differ from this version.

ABSTRACT

Lipid rafts, formed by sphingolipids and cholesterol within the membrane bilayer, are believed to have a critical role in signal transduction. $P2Y_2$ receptors are known to couple with G_q family G proteins, causing the activation of phospholipase C (PLC) and an increase in intracellular Ca^{2+} ($[Ca^{2+}]_i$) levels. In the present study, we investigated the involvement of lipid rafts in $P2Y_2$ receptor-mediated signaling and cell migration in NG108-15 cells. When NG108-15 cell lysates were fractionated by sucrose density gradient centrifugation, $G\alpha_{q/11}$ and a part of $P2Y_2$ receptors were distributed in a fraction where the lipid raft markers, cholesterol, flotillin-1 and ganglioside GM1 were abundant. Methyl-β-cyclodextrin (CD) disrupted not only lipid raft markers but also $G\alpha_{q/11}$ and $P2Y_2$ receptors in this fraction. In the presence of CD, $P2Y_2$ receptor-mediated phosphoinositide hydrolysis and $[Ca^{2+}]_i$ elevation were inhibited. Importantly, UTP-induced cell migration was inhibited by CD or the $G_{q/11}$-selective inhibitor YM254890. Moreover CD and YM254890 completely inhibited Rho-A activation. Downstream of Rho-A signaling, *i.e.*, stress fiber formation and phosphorylation of cofilin were also inhibited by CD or YM254890. However, UTP-induced phosphorylation of cofilin was not affected by the expression of p115-RGS which inhibits $G_{12/13}$ signaling pathway. This implies that UTP-induced Rho-A activation was relatively regulated by $G_{q/11}$ signaling pathway. These results suggest that lipid rafts are critical for $P2Y_2$ receptor-mediated $G_{q/11}$-PLC-Ca^{2+} signaling and this cascade is important for cell migration in NG108-15 cells.

Introduction

Recent studies indicate the existence of microdomains composed of sphingomyelin, glycosphingolipids and cholesterol on the cell surface. These microdomains are called “lipid rafts” because they are considered to float as liquid-ordered microdomains within the lipid-disordered glycerophospholipid membrane bilayer (Simons and Ikonen, 1997). Caveolae is also a well known microdomain, which is observed as the flask-shaped small pit on the cell surface, and has recently been considered as one of the lipid raft subtypes whose structure is stabilized by caveolin, an integral plasma membrane protein. It is reported that lipid rafts are important in diverse cellular responses, such as polarized protein sorting (Simons and Ikonen, 1997), cholesterol homeostasis (Schlegel et al., 2000) and cellular signaling (Vainio et al., 2002). Biochemically, lipid rafts are isolated as a non-ionic detergent-insoluble fraction (detergent-resistant membrane; DRM) (Brown and London, 2000). A wide range of proteins, such as glycosylphosphatidylinositol (GPI)-anchored proteins (Varma and Mayor, 1998) and fatty acid-modified (myristoylated or palmitoylated) proteins (Neumann-Giesen et al., 2004), have been reported to be partitioned in lipid rafts. Furthermore, many G protein-coupled receptor (GPCR)-mediated signaling molecules, such as heterotrimeric G proteins and their effectors (e.g. adenylyl cyclase, protein kinase C, Src family tyrosine kinase), are incorporated into lipid rafts (Foster et al., 2003). Therefore, the lipid rafts are now considered as a platform in GPCR-mediated cellular signaling which enables cells to transmit signals from external to internal spaces efficiently. Several pharmacological

JPET Fast Forward. Published on May 28, 2010 as DOI: 10.1124/jpet.110.167528
This article has not been copyedited and formatted. The final version may differ from this version.

tools are useful to analyze the involvement of lipid rafts in the cellular response. For example, methyl-β-cyclodextrin (CD) disrupts lipid raft structures because of its ability to bind and extract cholesterol from the cell membrane (Keller and Simons, 1998). Indeed, depletion of cholesterol by CD results in inhibition of bradykinin-induced phosphoinositide hydrolysis in A431 cells (Pike and Miller, 1998) or enhancement of β–adrenergic receptor or forskolin-stimulated cyclic AMP accumulation in rat cardiomyocytes (Rybin et al., 2000), suggesting the involvement of lipid rafts in the regulation of GPCR-mediated cellular signaling.

Extracellular purine/pyrimidine compounds mediate diverse physiological responses via activation of purine/pyrimidine receptors (Ralevic and Burnstock, 1998). P2 receptors, which preferentially bind adenine and uridine nucleotides, have been classified into P2X ($P2X_{1\text{-}7}$) and P2Y ($P2Y_{1, 2, 4, 6, 11, 12, 13, 14}$) receptors (North, 2002; Sak and Webb, 2002). While P2X receptor subtypes form the non-selective cation channels, P2Y receptor subtypes couple with heterotrimeric G proteins to regulate the effector systems including phospholipase C (PLC) and adenylyl cyclase (AC). The neuroblastoma x glioma hybrid NG108-15 cell line shows diverse cellular responses to purine/pyrimidine compounds, such as elevations in intracellular Ca^{2+} ($[Ca^{2+}]_i$) via G_q-PLC (Matsuoka et al., 1995). Among P2Y receptors, the $P2Y_2$ receptor has been shown to couple with G_q family G proteins, causing the activation of PLC-β isoforms and an increase in $[Ca^{2+}]_i$ (Lustig et al., 1993). Recently, the $P2Y_2$ receptor has been shown to couple with not only $G_{q/11}$ but also $G_{i/o}$ and $G_{12/13}$ when the receptor is associated with $\alpha_V\beta_3/\beta_5$ integrins through the Arg-Gly-Asp (RGD) domain in its first

extracellular loop in human 1321N1 astrocytoma cells (Erb et al., 2001; Liao et al., 2007). By interacting with $\alpha_V\beta_3/\beta_5$ integrins, the $P2Y_2$ receptor effectively mediates migration of 1321N1 human astrocytoma cells. In addition to this cell line, the $P2Y_2$ receptor also regulates cell migration in epidermal keratinocytes, lung epithelial carcinoma cells and smooth muscle cells (Greig et al., 2003). Studies on phagocytic removal of apoptotic cells revealed that nucleotides released by apoptotic cells act as a 'find-me' signal and that the $P2Y_2$ receptor acts as a sensor of the nucleotides to promote migration of cells such as monocytes (Elliott et al., 2009). Moreover, chemotaxis is important for many physiological and pathological processes and nucleotides play important roles as chemoattractants in many cells (Elliott et al., 2009).

Cell migration via the $P2Y_2$ receptor has been reported, however, the detailed regulatory mechanism is not well known. As mentioned above, lipid rafts are involved in GPCR-mediated cellular signaling as a platform. In the present study, we examined the role of lipid rafts in $P2Y_2$ receptor-mediated signaling in detail, focusing on cell migration signaling, in NG108-15 cells.

JPET Fast Forward. Published on May 28, 2010 as DOI: 10.1124/jpet.110.167528
This article has not been copyedited and formatted. The final version may differ from this version.

Materials and Methods

Materials

DMEM, FCS ATP, UTP, benzoyl benzoic ATP (BzATP), lysophosphatidic acid (LPA), cholesterol and anti-β-tubulin antibody were obtained from Sigma Aldrich (St. Louis, MO, USA). HAT supplement was purchased from Gibco BRL (Rockville, MD, USA). Tert-butyl-hydroquinone (tBuBHQ) and fura-2/acetoxymethylester (Fura-2/AM) were obtained from Wako Pure Chemicals (Tokyo, Japan). (R)-(+)-*trans*-N-(4-Pyridyl)-4-(1-aminoethyl)-cyclohexanecarboxamide (Y-27632) was obtained from Calbiochem (La Jolla, CA, USA). YM254890 was kindly provided by Astellas Pharma Inc. (Tokyo, Japan). [^{3}H]-Myo-inositol was obtained from American Radiochemicals, Inc. (St. Louis, MO, USA). Antibody for integrin α_v blocking antibody (P2W7) was purchased from Santa Cruz Biotechnology (Santa Cruz, CA, USA). Antibodies for $G\alpha_{q/11}$ and $P2Y_2$ receptor were purchased from Daiichi Pure Chemicals Co. Ltd. (Tokyo, Japan) and Alomone lab (Jerusalem, Israel), respectively. Antibodies for phospho-cofilin (Ser3) (77G2) was purchased from Cell Signaling Technology (Beverly, MA, USA). Horseradish peroxidase (HRP)-conjugated choleratoxin B subunit and HRP-conjugated anti-rabbit IgG and were obtained from Calbiochem (La Jolla, CA, USA) and Cell Signaling Technology (Beverly, MA, USA), respectively. HRP-conjugated anti-mouse IgG, Immobilon P, ECL and Hyperfilm ECL were purchased from GE Healthcare UK Ltd. (Buckinghamshire, England). Adenovirus encoding the amino terminal region containing the regulator of G protein

JPET Fast Forward. Published on May 28, 2010 as DOI: 10.1124/jpet.110.167528
This article has not been copyedited and formatted. The final version may differ from this version.

signaling (RGS) domain of p115-RhoGEF (p115-RGS; amino acids 1-252) was kindly given from Dr. H. Kurose (Kyushu University, Fukuoka, Japan). All other chemicals or drugs were of reagent grade or of the highest quality available.

Cell culture

NG108-15 cells were grown in high glucose DMEM supplemented with 10% (v/v) FCS and HAT supplement (100 μM hypoxanthine, 1 μM aminopterin and 16 μM thymidine), and maintained in a humidified atmosphere of 5% CO_2 in air at 37°C.

Measurement of lactate dehydrogenase (LDH) activity

NG108-15 cells in the 12-well plates were washed twice with modified Tyrode's solution (137 mM NaCl, 2.7 mM KCl, 1 mM $MgCl_2$, 0.18 mM $CaCl_2$, 5.6 mM glucose, 10 mM HEPES, pH 7.4), and treated with various concentrations of CD for 30 min at 37°C. The incubation medium was collected, and the LDH activity was assayed using a commercially available kit (Wako Pure Chemical Ltd, Tokyo, Japan).

Measurement of cholesterol content

The cholesterol content was examined by using a commercially available kit (Wako Pure Chemical Ltd, Tokyo, Japan). NG108-15 cells were detached from 150 mm diameter dishes and washed twice, and finally suspended with modified Tyrode's solution. Suspended cells (1.8×10^6 cells) in 1.5 ml tubes were treated with various

JPET Fast Forward. Published on May 28, 2010 as DOI: 10.1124/jpet.110.167528
This article has not been copyedited and formatted. The final version may differ from this version.

concentrations of CD for 30 min at 37°C. After incubation, cells were centrifuged at 15,000 x g for 5 min at 4°C, and the supernatants were collected as the fractions containing the released cholesterol from cellular membranes. Total lipids were extracted from cell pellets with $CHCl_3$/methanol/H_2O, and were regarded as the fraction containing the intracellular cholesterol. In the case of analysis to measure the time course of cholesterol content in the plasma membrane after CD treatment, membrane fractions were collected from cells grown in 6-well plates that were incubated for 0, 1, 3, 5, 10, 18 hr after 10 mM CD pretreatment for 30 min. Following incubation, cells were lysed and sonicated in lysis buffer (20 mM KCl, 2.5 mM $MgCl_2$, 1 mM EDTA, 1 mM DTT, 1 mM Na_3VO_4, 5 mM $Na_4P_2O_7$, 1 mM PMSF, 10 μg/ml aprotinin, 10 μg/ml leupeptin/antipain, 20 mM HEPES, pH 7.4). Nuclei were precipitated by centrifugation at 600*g* for 10 min at 4°C. The supernatant was centrifuged at 15,000*g* for 30 min at 4°C and the remaining pellet (plasma membrane fraction) was resuspended in H_2O. In the case of analysis to measure cholesterol in a fraction separated by sucrose-density gradient, 100 μl of each fraction was used and expressed as cholesterol content (μg/fraction).

Isolation of raft fractions and immunoblotting

Raft fractions were separated by the sucrose gradient method described previously (Sugama et al., 2005). NG 108-15 cells grown on 150 mm dishes were suspended, washed twice, and finally suspended in modified Tyrode's solution. The cells were

JPET Fast Forward. Published on May 28, 2010 as DOI: 10.1124/jpet.110.167528
This article has not been copyedited and formatted. The final version may differ from this version.

incubated with or without 10 mM CD for 30 min at 37°C, washed twice, and lysed with 1 ml of ice-cold lysis buffer (0.1% (v/v) Triton X-100, 50 mM Tris-HCl, 50 mM NaCl, 5 mM EDTA, 50 mM NaF, 1 mM Na_3VO_4, 5 mM $Na_4P_2O_7$, 1 mM PMSF, 10 μg/ml aprotinin, 10 μg/ml leupeptin/antipain, pH 7.6). Lysates were sonicated on ice and incubated with constant rotation at 4°C for 1 hr. Lysates (1 ml) were mixed with 3 ml of 60% (w/v) sucrose in STE buffer (50 mM Tris-HCl, 50 mM NaCl, 5 mM EDTA, and 1 mM Na_3VO_4, pH 7.6) and overlaid with 4 ml of 35% (w/v) sucrose and 4 ml of 5% (w/v) sucrose. Centrifugation was performed at 200,000*g* for 16 hr at 4°C with a Beckman SW41Ti rotor. Fractions of 1 ml were collected from the top of the gradients, and a total of 12 fractions were kept at -80°C for subsequent studies.

Samples were mixed with 3 x Laemmli sample buffer and denatured by heating at 95°C for 5 min. In the case of the $P2Y_2$ receptors, the samples were denatured at room temperature overnight. Standard immunoblotting was performed, and blots were probed for flotillin-1 (1:300), $G\alpha_{q/11}$ (1:2,000) and $P2Y_2$ receptor (1:200). For the detection of GM1, dot blotting was performed using HRP-conjugated choleratoxin B subunit (Sigma-Aldrich, final 10 ng/ml).

MTT assay

NG108-15 cells grown in the 96-well plates coated with poly-L-lysine (100 ng/ml) were treated with various concentrations of CD for 30 min or 18 hr at 37°C. Following removal of the incubation medium, 100 μl of EMEM-HEPES or MTT solution was

JPET Fast Forward. Published on May 28, 2010 as DOI: 10.1124/jpet.110.167528
This article has not been copyedited and formatted. The final version may differ from this version.

added and cells were incubated for 4 hr at 37°C. After removal of the medium, 100 µl of DMSO was added and the absorbance measured using the absorptiometer (Sunrise, Tecan, Austria).

Cell migration assay

Cell migration assays were performed with 8-µm pore size cell culture inserts (BD bioscience) by the method previously described (Wang et al., 2005) with a slight modification. The cells (5×10^4) were pretreated with or without 10 mM CD for 30 min or 1 µM YM254890 for 30 min, and suspended in 100 µl of serum-free DMEM supplemented with 100 µM hypoxanthine, 1 µM aminopterin and 16 µM thymidine and placed in the inserts (upper chamber). CD was washed out, and the medium was replaced with a new medium. YM254890 was kept in the medium during the following 18 hr-incubation. The lower chamber was filled with 600 µl of serum-free medium with or without 100 µM UTP. Cells were allowed to migrate under the incubation for 18 hr at 37°C. Cells migrating to the lower side of the membrane were fixed with 4% (v/v) paraformaldehyde (PFA) and stained with 1 ng/ml Hoechst 33258. Photographs of all fields were taken and the number of migrating cells was counted.

Measurement of phosphoinositide hydrolysis

Phosphoinositide hydrolysis was determined as described previously with slight

modifications (Nakahata et al., 1990). Cells grown in 12-well plates were labeled with [^{3}H]-inositol (2 μCi/ml) in DMEM for 18-24 hr before experimentation. Cells were washed twice, and incubated in modified Tyrode's solution with or without the various concentrations of CD for 30 min at 37°C. After incubation, cells were washed twice and incubated in modified Tyrode's solution containing 10 mM LiCl for 10 min at 37°C. Cells were stimulated with agonists for 10 min at 37°C, and the reaction was terminated by addition of 5% (v/v) trichloroacetic acid (TCA) after aspiration of the incubation medium. Total amounts of [^{3}H]-inositol phosphates in the ether-washed TCA extract were separated using an anion exchange column (AG 1X-8, formate form). The [^{3}H]-radioactivity in the eluates was measured using a liquid scintillation counter.

Measurement of $[Ca^{2+}]_i$

Increases in $[Ca^{2+}]_i$ were examined by monitoring the intensity of Fura-2 fluorescence as described previously (Sugama et al., 2005). Cells were loaded with 1 μM Fura-2/AM for 15 min at 37°C, washed twice and suspended at 0.5-1 x 10^6 cells/ml in modified Tyrode's solution. The cell suspension was placed in a 1.5 ml quartz cell and constantly stirred at 37°C. The increase in $[Ca^{2+}]_i$ was determined by measuring the fluorescence intensity of Fura-2 (excitation wave length at 340 and 380 nm and emission wave length at 510 nm) using a fluorescence spectrophotometer (Hitachi, F-2000). $[Ca^{2+}]_i$ levels were calculated using the K_d value of Fura-2 to Ca^{2+} as 224 nM.

JPET Fast Forward. Published on May 28, 2010 as DOI: 10.1124/jpet.110.167528
This article has not been copyedited and formatted. The final version may differ from this version.

Preparation of CD-cholesterol complex

CD-cholesterol complex was prepared by modifying the method described by Zidovetzki and Levitan (2007). CD (10 mM) solution in serum free DMEM was added to the dried cholesterol equivalent of 100 mM (CD: cholesterol molar ratios of 1:10). They were vortexed, sonicated in bath sonicator for 2 min, and incubated overnight in a shaking bath at 37℃. Immediately before using this solution, excess cholesterol crystals were removed by 0.45 μm syringe filter (Milipore, Bedford, MA, USA). This CD solution was considered to be 100% saturated with cholesterol. To prepare different concentrations of cholesterol combined with 10 mM CD, this 100% saturated 10 mM CD-cholesterol solution was mixed with various amounts of 10 mM CD without cholesterol. Briefly, 75% saturated CD-cholesterol solution was prepared by mixing with 3:1 (100% saturated 10 mM CD-cholesterol solution: 10 mM CD alone), and 50% saturated CD-cholesterol solution was prepared by mixing with 1:1.

Rho activation assay

Rho activity was assessed by using the Rho activation assay kit (Cat. # BK036, Cytoskeleton) according to the manufacture's instructions. Briefly, cells were seeded onto 60-mm dishes (1 x 10^6 cells) and cultured for 24 hr at 37°C. The medium was replaced with serum-free medium and incubated for 48 hr before experimentation. After drug exposure, cells were lysed in 0.5 ml of lysis buffer and centrifuged at 1,000

rpm for 2 min at 4°C. GST fusion-Rho binding domain (RBD) of Rhotekin-glutathion agarose (50 μg) that only recognizes GTP-bound Rho, was added to 450 μl of supernatant and incubated for 1 hr at 4°C. The beads were precipitated by centrifugation at 3,000 rpm for 30 s at 4°C and washed once with wash buffer. Finally, the beads were resuspended in 20 μl of 2 x Laemmli's sample buffer and heated at 95°C for 2 min. Immunoblotting was performed using an antibody against Rho-A (1:500). The density of the band was analyzed by densitometry (Image J 1.36, National Institutes of Health).

Actin stress fiber formation

NG 108-15 cells were plated on glass coverslips and cultured for 48 hr at 37°C. Cells were pretreated with or without 10 mM CD for 30 min, 1 μM YM254890 for 15 min or 5 μg/ml PTX for 24 hr and stimulated with 100 μM UTP for 30 min in serum-free medium. Cells were washed in PBS, fixed with 4% (v/v) PFA for 15 min, treated with 0.1% Triton X-100 for 10 min, and rinsed with PBS. Cells were incubated with 1% bovine serum albumin (BSA) for 1 hr at 37°C. For staining of actin, cells were incubated with 5 U/ml rhodamine-phalloidin in PBS with 5% BSA for 2 hr at 37°C and washed with PBS. Coverslips were mounted on glass slides in fluorescent mounting medium (Dako Cytomation) and examined using the confocal laser scanning microscope (FV 1000, Olympus).

JPET Fast Forward. Published on May 28, 2010 as DOI: 10.1124/jpet.110.167528
This article has not been copyedited and formatted. The final version may differ from this version.

Detection of cofilin phosphorylation

Cells were seeded onto 6-well plates (2 x 10^5 cells) and cultured for 24 hr at 37°C. The medium was replaced with serum-free medium and cells were incubated for 24 hr before experimentation. After stimulation, cells were lysed in 0.3 ml of Laemmli's sample buffer (75 mM Tris-HC1, 2% SDS, 15% g1ycero1, 3% 2-mercaptoethano1, 0.003% bromophenol blue, pH 6.8). Lysates were heated at 95℃ for 5 min to denature protein. Equal volumes of samples were resolved by 11% SDS-PAGE, and transferred onto polyvinylidene difluoride (PVDF) membranes (Hybond P, Amersham) using the semi-dry blotting method. After blocking membranes with 3% non-fat milk in TBST (10 mM Tris, 100 mM NaCl, 0.1% Tween 20, pH 7.4) for 1 hr at room temperature, membranes were incubated with primary antibodies against phospho-cofilin (1:500) in TBST containing 3% non-fat milk overnight at 4^{o}C. After several washes with TBST, membranes were incubated with horseradish peroxidase (HRP)-linked rabbit IgG (1:50,000). Bands were visualized using the ECL system (GE Healthcare) by exposing its chemiluminescence to Hyperfilm ECL (GE Healthcare). The density of the band was analyzed by densitometry (Image J 1.36, National Institutes of Health).

Statistical analysis

All results are expressed as the mean ± S.E.M., and statistical differences of values were determined by one-way analysis of variance with Dunnett's or Tukey's Kramer *post hoc* tests for multiple comparisons.

JPET Fast Forward. Published on May 28, 2010 as DOI: 10.1124/jpet.110.167528
This article has not been copyedited and formatted. The final version may differ from this version.

Results

$G\alpha_{q/11}$ and a part of $P2Y_2$ receptors are localized in lipid rafts

First, we tried to determine the suitable concentration of CD to deplete cholesterol in plasma membranes. When NG108-15 cells were incubated with various concentrations of CD for 30 min at 37°C, CD extracted cholesterol from the plasma membranes into the incubation medium in a concentration-dependent manner with an EC_{50} value of approximately 5.6 mM (Fig. 1A). Because cholesterol is one of the major components in plasma membranes, the reduction of cholesterol from plasma membranes by CD would cause a decrease in cell viability. In fact, the severe depletion of cholesterol is reported to cause cytotoxicity (Iwabuchi et al., 1998). Therefore, we examined cell viability after CD treatment by determining the release of lactate dehydrogenase (LDH) activity from cells into the incubation medium. CD at a concentration of 20 mM resulted in a 56.6 $\pm$ 3% (n=3) increase in LDH release compared with untreated cells, but less LDH was released into the medium when concentrations of CD up to 10 mM were used (Fig. 1B). For this reason, we used CD at a concentration of 10 mM or lower in all subsequent experiments. To evaluate the distribution of the signaling molecules underlying $P2Y_2$ receptor signaling, we tried to isolate the raft fraction by sucrose density gradient centrifugation (Fig. 2). The majority of cholesterol was concentrated within fraction 4/5, which disappeared upon pretreatment of cells with CD (Fig. 2A). Furthermore, flotillin-1 and GM1 were also concentrated in fraction 4/5, and they were moved to the higher sucrose density fraction by CD-treatment at 10 mM for 30 min (Fig. 2B and 2C). We therefore defined the

JPET Fast Forward. Published on May 28, 2010 as DOI: 10.1124/jpet.110.167528
This article has not been copyedited and formatted. The final version may differ from this version.

fraction 4/5 as the raft fraction. We next investigated the localization of a heterotrimeric G protein $G\alpha_{q/11}$ and the $P2Y_2$ receptor. While $G\alpha_{q/11}$ was enriched in the raft fraction from control cells, CD disrupted the localization of $G\alpha_{q/11}$ and moved it into the higher sucrose density fractions (Fig. 2D). $P2Y_2$ receptors were partially distributed in the raft fraction, and the lipid raft-associated $P2Y_2$ receptor moved to the higher sucrose density fraction after CD-treatment (Fig. 2E). These results suggest that $G\alpha_{q/11}$ and a part of $P2Y_2$ receptors are localized in lipid rafts in NG 108-15 cells.

Inhibitory effect of CD on UTP-induced cell migration

First, we investigated the optimal condition of CD treatment for migration assays. When we examined cytotoxicity using the MTT assay, treatment with CD for 18 hr caused a decrease in cell viability at all concentrations used (Fig. 3A). In contrast, the treatment with CD for 30 min and incubation for an additional 18 hr after removal of CD resulted in no cytotoxicity and a long-term reduction in cholesterol content of the plasma membranes (Fig. 3A and 3B).

Next, we investigated whether lipid rafts participated in UTP-induced cell migration, which is the unique physiological function of $P2Y_2$ receptors. Because it is considered that this migration assay reflects accumulative reaction and the inhibitory effect is more obvious when cells are incubated for some long time, the migration assay was also performed for 18 hr incubation as performed previously by Wang, et al (2005). After an 18 hr incubation of cells in the upper chamber in the presence or absence of UTP in the lower chamber, cells migrating to the lower side of the membrane were

JPET Fast Forward. Published on May 28, 2010 as DOI: 10.1124/jpet.110.167528
This article has not been copyedited and formatted. The final version may differ from this version.

visualized by staining with Hoechst 33258 (Fig. 3C) and the number of migrated cells was counted. As a result, UTP significantly promoted cell migration (Fig. 3D). Furthermore, UTP-induced increase in cell migration was completely suppressed by pretreatment with CD (Fig. 3D).

Involvement of $G_{q/11}$ in UTP-induced cell migration

As reported previously, depletion of cholesterol by CD resulted in inhibition of bradykinin-induced phosphoinositide hydrolysis in A431 cells (Pike and Miller, 1998). Because $P2Y_2$ receptors are known to associate with $G_{q/11}$ and cause various responses via $G_{q/11}$, we suspected that the inhibition of UTP-induced cell migration by disruption of lipid rafts was due to inhibition of $G_{q/11}$–mediated signaling. To examine this possibility, we investigated the effect of CD on phosphoinositide hydrolysis as an index of $G_{q/11}$ signaling. CD itself had little effect on the total amount of [^{3}H]-inositol labeled lipids (data not shown) and the resting level of [^{3}H]-inositol phosphates (IPs) (Fig. 4A), suggesting that labeling efficiency of phosphoinositides by [^{3}H]-inositol was not affected by CD-treatment. However, UTP (100 μM)-induced phosphoinositide hydrolysis was clearly inhibited by CD-treatment in a concentration-dependent manner (Fig. 4A). We next examined the effect of CD on $[Ca^{2+}]_i$ elevation. ATP (100 μM) caused transient $[Ca^{2+}]_i$ elevation in Fura-2-loaded cells, which was suppressed by the pretreatment of cells with 10 mM CD for 30 min (Fig. 4B and 4C). In contrast, $[Ca^{2+}]_i$ elevation induced by tBuBHQ (10 μM), an inhibitor of Ca^{2+}-ATPase at the endoplasmic reticulum (ER) (Moore et al., 1987), was little affected by CD-treatment, suggesting

JPET Fast Forward. Published on May 28, 2010 as DOI: 10.1124/jpet.110.167528
This article has not been copyedited and formatted. The final version may differ from this version.

that the inhibitory effect of CD on $[Ca^{2+}]_i$ increase is not due to the reduction in Ca^{2+} uptake into the ER. While the $P2Y_2$ receptor agonist, UTP (100 μM), caused a transient elevation in $[Ca^{2+}]_i$, the $P2X_7$ receptor agonist BzATP (100 μM) induced a sustained elevation in $[Ca^{2+}]_i$ in normal cells. Although BzATP-induced $[Ca^{2+}]_i$ elevation was slightly facilitated by CD, UTP-induced $[Ca^{2+}]_i$ elevation was largely inhibited. These results suggest that the inhibitory effect of CD on UTP-induced $[Ca^{2+}]_i$ elevation might be due to the suppression of the $P2Y_2$ receptor-$G_{q/11}$-mediated signaling pathway. Then, we investigated whether $G_{q/11}$ was involved in the UTP-induced cell migration. As observed in case of CD treatment, UTP-induced cell migration was completely suppressed to control levels in the presence of 1 μM YM 254890, a specific inhibitor of $G_{q/11}$ (Fig. 4D) (Takasaki et al., 2004). These results suggest that $P2Y_2$ receptor-mediated $G_{q/11}$ signaling at lipid rafts is essential for cell migration in NG108-15 cells.

CD-exogenous cholesterol complex failed to inhibit UTP-induced cell migration

To confirm that the inhibition of G_q signaling and cell migration by CD was due to cholesterol depletion but not non-specific effect, we tried to determine the cellular cholesterol level and UTP-induced phosphoinositide hydrolysis after the treatment with CD alone or with CD-cholesterol complex. While 10 mM CD solution without exogenous cholesterol (0% saturation) decreased cellular cholesterol contents, 50% saturated 10 mM CD-cholesterol solution scarcely decreased the cellular cholesterol contents in NG 108-15 cells (Fig. 5A). The inhibition of UTP-induced

JPET Fast Forward. Published on May 28, 2010 as DOI: 10.1124/jpet.110.167528
This article has not been copyedited and formatted. The final version may differ from this version.

phosphoinositide hydrolysis by CD was attenuated by exogenous cholesterol in a concentration-dependent manner (Fig. 5B). Furthermore, 75% saturated 10 mM CD-cholesterol did not inhibit the UTP-induced cell migration (Fig. 5C). These data strongly suggest that the inhibition of $P2Y_2$ receptor-mediated G_q signaling and cell migration by CD was due to cholesterol depletion.

On the other hand, the result in Fig. 3B shows a gradual increase in cholesterol content after CD treatment. Hence, to investigate the relationship between cholesterol content and $P2Y_2$ receptor-mediated signaling after CD treatment, we measured the UTP-induced $[Ca^{2+}]_i$ elevation 18 hr after 30-min pre-treatment with CD. Although cholesterol contents were recovered 18 hr after 30-min pre-treatment with CD, the UTP-induced $[Ca^{2+}]_i$ elevation was not completely recovered (Fig. 5D), suggesting that the integrity of the lipid rafts was still disrupted following 18 hr incubation after 30-min pre-treatment with CD and some factors are required to recover their function once cellular cholesterol is extracted by CD.

$G_{q/11}$-dependent Rho-A activation

Fig. 4 indicates the possible involvement of $G_{q/11}$ in $P2Y_2$ receptor-mediated cell migration. On the other hand, Rho-A, which is the member of the Rho family of small GTPase, is required for cytoskeletal reorganization and cell migration (Xu et al., 2003). Therefore, to investigate this signal transduction pathway in more detail, we examined the effect of $G_{q/11}$ on Rho-A activation. Interestingly, UTP-induced Rho-A activation was inhibited by CD or YM254890, but weakly affected by anti-integrin α_V antibodies

JPET Fast Forward. Published on May 28, 2010 as DOI: 10.1124/jpet.110.167528
This article has not been copyedited and formatted. The final version may differ from this version.

(Fig. 6). These data suggest that UTP-induced Rho-A activation is regulated by $G_{q/11}$.

$G_{q/11}$-dependent stress fiber formation

To assess the involvement of $P2Y_2$ receptor-$G_{q/11}$ signaling in Rho-A activation, we investigated the effect of UTP on stress fiber formation. Actin stress fibers were observed by stimulating NG108-15 cells with UTP (Fig. 7B), which was reversed by pretreatment with 10 mM CD or 1 μM YM254890 (Fig. 7C and 7D). In addition, stress fiber formation over a population of cells was quantitated (Fig. 7F). Judging from this result, it is considered that the inhibition of stress fiber formation by CD was not partial. This is consistent with the results that CD largely blocked the UTP-induced Rho activation (Fig. 6). However, PTX, which inactivates the receptor-mediated $G_{i/o}$ function, did not affect the formation (Fig. 7E). These data further support the idea that $G_{q/11}$ is involved in Rho-A activation.

$G_{q/11}$-dependent phosphorylation of cofilin

To further access the involvement of $G_{q/11}$ in Rho-A signaling pathway, we examined the influence of the phosphorylation of cofilin, which regulates stress fiber formation (Ohashi et al., 2000). UTP induced robust cofilin phosphorylation, which was inhibited by YM254890 and CD, but not by PTX (Fig. 8A, 8B, 8C and 8D), as was the case in stress fiber formation. Phosphorylation of cofilin was partially inhibited by anti-integrin α_V antibodies (Fig. 8C and 8D). Since YM254890 did not inhibit phosphorylation of cofilin when NG 108-15 cells were stimulated by lysophosphatidic

JPET Fast Forward. Published on May 28, 2010 as DOI: 10.1124/jpet.110.167528
This article has not been copyedited and formatted. The final version may differ from this version.

acid (LPA) (Fig. 8E and 8F), which is considered to induce Rho-A activation via $G_{12/13}$, it is suggested that YM254890 specifically inhibits $G_{q/11}$ signaling. To further clarify the G proteins involved in UTP-induced phosphorylation of cofilin, we investigated the involvement of $G_{12/13}$ in the UTP-induced Rho-A signaling by using adenovirus encoding the amino terminal regions containing RGS domain of p115 RhoGEF (p115-RGS; amino acid 1-252), which specifically inhibits $G\alpha_{12/13}$ function (Honma et al., 2006). While the expression of p115-RGS resulted in a significant attenuation of LPA-induced phosphorylation of cofilin, it did not affect UTP-induced phosphorylation of cofilin (Fig. 8G, 8H and 8I). These results (Fig. 8A-8I) suggest that UTP-induced phosphorylation of cofilin is regulated by $G_{q/11}$ rather than $G_{12/13}$.

It is known that cofilin is phosphorylated by LIM domain kinase (LIMK) that is activated downstream of Rho-A, Rac1 or Cdc42 (Edwards et al., 1999; Ohashi et al., 2000). The activity of LIMK is regulated by ROCK, which is an effector molecule of Rho-A, or PAK1, which is an effector molecule of Rac1 and Cdc42 (Edwards et al., 1999; Ohashi et al., 2000). When NG 108-15 cells were stimulated with UTP, the phosphorylation of cofilin was potently inhibited by Y27632, a ROCK inhibitor (Fig. 8J and 8K). Because phosphorylation of cofilin was regulated by ROCK and $G_{q/11,}$ it was speculated that UTP-induced Rho-A activation was regulated by the $P2Y_2$ receptor-$G_{q/11}$ signaling pathway.

JPET Fast Forward. Published on May 28, 2010 as DOI: 10.1124/jpet.110.167528
This article has not been copyedited and formatted. The final version may differ from this version.

Discussion

In the present study, we have clearly demonstrated that the $P2Y_2$ receptor and $G_{q/11}$ are present in the cholesterol-rich lipid rafts that are required for effective signal transduction and this signal transduction via $G_{q/11}$ is essential for cell migration in NG 108-15 cells. Many GPCRs and their effector systems have been shown to exist in microdomains, including caveolae, this is the first direct demonstration that the $P2Y_2$ receptors are localized in lipid rafts where their physiological function is regulated.

It has been shown that ATP interacts with $P2X_7$ and $P2Y_2$ receptors expressed in NG108-15 cells (Watano et al., 2002). CD is reported to extract the cholesterol followed by disruption of the cholesterol-dependent lipid rafts on the plasma membrane in NG108-15 cells. In this study, CD treatment inhibited the UTP-induced, but not BzATP-induced, $[Ca^{2+}]_i$ elevation, suggesting that CD-treatment inhibits the $P2Y_2$ receptor-mediated, but not the $P2X_7$-mediated, signaling pathway. On the other hand, tBuBHQ-induced $[Ca^{2+}]_i$ elevation was unaffected by CD-treatment, suggesting that CD did not decrease the Ca^{2+} levels in the ER and that CD-induced inhibition of the $P2Y_2$ receptor-mediated signaling pathway occurred upstream of Ca^{2+} release from the ER. In fact, CD suppressed UTP-induced phosphoinositide hydrolysis in a concentration-dependent manner, indicating that $P2Y_2$ receptor-mediated $G_{q/11}$-PLC activation would be interrupted by CD. Interestingly, we have also shown that CD inhibited $P2Y_2$ receptor-mediated PLC activation in PC12 cells (Sugama et al., 2005).

Toseli *et al.* (Toselli et al., 2001) reported that NG 108-15 cells possess lipid rafts, but not caveolae. The results in Fig. 2 provide strong evidence that the signaling

JPET Fast Forward. Published on May 28, 2010 as DOI: 10.1124/jpet.110.167528
This article has not been copyedited and formatted. The final version may differ from this version.

molecule complex for the $P2Y_2$ receptor exists in lipid rafts. The lipid raft marker molecules, ganglioside GM1 and flotillin-1, were co-localized in the fraction 4/5. CD reduced the levels of these molecules in the fraction, suggesting that the depletion of cholesterol from the plasma membranes would effectively disrupt the lipid raft composition followed by the re-distribution of these molecules to non-raft compartments. On the other hand, $G\alpha_{q/11}$ and a part of the $P2Y_2$ receptor were found in raft fraction derived from CD-untreated cells. This may suggest the effective coupling between $P2Y_2$ receptors and $G_{q/11}$ in the cholesterol-rich lipid raft compartment. Consistent with our results, $G_{q/11}$ is reported to be localized in lipid rafts including caveolae (Oh and Schnitzer, 2001), because $G\alpha$ subunit interacts with membrane lipids via saturated acyl chains (typically myristate and/or palmitate) covalently attached at the amino terminus of this molecule (Morris and Malbon, 1999). In contrast to $G\alpha_{q/11}$, which was detected in raft fraction, $P2Y_2$ receptor showed more broad distribution in both raft and non-raft fractions (Fig. 2E). CD-treatment fully inhibited $P2Y_2$ receptor-mediated PLC activation and $[Ca^{2+}]_i$ mobilization accompanied by reduced $P2Y_2$ receptor levels in raft fractions, indicating that only lipid raft-associated $P2Y_2$ receptors would be functional to couple with the $G_{q/11}$-PLC-Ca^{2+} pathway.

Interestingly, cell migration was regulated by $G_{q/11}$ in NG 108-15 cells and the number of migrated cells was completely decreased by pretreatment with YM254890 (Fig. 4D). This indicates that $G_{q/11}$ has a critical role in cell migration in NG 108-15 cells. Indeed, Rho-A activation was totally inhibited by YM254890. Downstream of

JPET Fast Forward. Published on May 28, 2010 as DOI: 10.1124/jpet.110.167528
This article has not been copyedited and formatted. The final version may differ from this version.

Rho-A signaling, *i.e.*, stress fiber formation (Fig. 7D) and phosphorylation of cofilin (Fig. 8A and 8B) were also inhibited. However, YM254890 did not inhibit LPA-induced phosphorylation of cofilin (Fig. 8E and 8F). On the other hand, UTP-induced phosphorylation of cofilin was not affected by p115-RGS even though LPA-induced phosphorylation of cofilin was inhibited (Fig. 8G, 8H and 8I). In addition, the phosphorylation of cofilin was inhibited by Y27632, a ROCK inhibitor (Fig. 8J and 8K). These data suggest that $G_{q/11}$ is required for transmit the signal from $P2Y_2$ receptor to Rho-A in NG 108-15 cells. It has been demonstrated that the UTP-induced cell migration requires interaction with $\alpha_V\beta_3/\beta_5$ integrins (Wang et al., 2005). Our results are consistent with this report (Wang et al., 2005), *i.e.*, phosphorylation of cofilin was inhibited by pretreatment with anti-integrin α_V antibody (Fig. 8C and 8D), indicating the involvement of $\alpha_V\beta_3/\beta_5$ integrins. Judging from these results, we assumed that the $P2Y_2$ receptor-$G_{q/11}$ signaling pathway may activate integrins, resulting in the activation of Rho-A. Nevertheless, Rho-A activation was not affected by anti-integrin α_V antibody, suggesting that $\alpha_V\beta_3/\beta_5$ integrins may transmit the signal to Rac1 or Cdc42 because cofilin is regulated by not only Rho-A but also Rac1 or Cdc42 (Edwards et al., 1999; Ohashi et al., 2000). Hence, these results indicate that $P2Y_2$ receptor-mediated activation of Rho-A is relatively $G_{q/11}$-specific in NG 108-15 cells. This $P2Y_2$ receptor-$G_{q/11}$ mediated Rho-A activation is a new signal transduction pathway. We suspected that $G\alpha_q$-dependent Rho GEF, for example LARG (Booden et al., 2002) and p63 Rho GEF (Rojas et al., 2007), mediated the UTP-induced Rho-A activation in NG 108-15 cells. Recently, the crystal structure of

JPET Fast Forward. Published on May 28, 2010 as DOI: 10.1124/jpet.110.167528
This article has not been copyedited and formatted. The final version may differ from this version.

$G\alpha_q$-p63 Rho GEF-Rho A was determined (Lutz et al., 2007). Moreover, $G\alpha_q$ was found to directly activate p63 Rho GEF, resulting in the activation Rho-A (Rojas et al., 2007).

It is not clear how the $P2Y_2$ receptor is retained in the lipid rafts. A possible mechanism to regulate the localization of molecules is glycosylation. Kohno *et al.* (Kohno et al., 2002) suggested that sphingosine 1-phosphate receptor Edg-1 existed in the caveolae and that the mutated form of non-glycosylated N30D-Edg-1 existed in the broad membrane fractions separated by sucrose density gradient centrifugation. It has been shown that the human $P2Y_2$ receptor has two N-glycosylation sites at 9 and 13 residues (Lustig et al., 1993; Erb et al., 2001). Thus, further studies are necessary to clarify whether these glycosylation sites are essential for the distribution of the $P2Y_2$ receptor in lipid rafts. Recent studies indicated that human $P2Y_2$ receptors possess several functional domains, *i.e.,* one RGD integrin-binding sequence in the first extracellular loop (Liao et al., 2007) and two proline-rich Src homology 3 (SH3) domain binding sites (PXXP motif) in the carboxy terminal tail (Liu et al., 2004). The putative amino acid sequence of $P2Y_2$ receptor cloned from NG 108-15 cells (Accession No. AAA39871.1) showed the presence of one RGD sequence and one SH3 domain binding site. In human $P2Y_2$ receptors, expression of $P2Y_2$ receptors replaced with an RGE sequence from an RGD sequence did not change G_q-mediated signaling (Liao et al., 2007). Furthermore, a mutant $P2Y_2$ receptor lacking two PXXP motifs still stimulated $[Ca^{2+}]_i$ mobilization (Liu et al., 2004), suggesting that both the RGD sequence and the SH3-binding sites would not be important for $G_{q/11}$-mediated Ca^{2+}

JPET Fast Forward. Published on May 28, 2010 as DOI: 10.1124/jpet.110.167528
This article has not been copyedited and formatted. The final version may differ from this version.

signaling and localization of the $P2Y_2$ receptor in lipid rafts. It might be possible that there are unidentified motifs in the $P2Y_2$ receptors which enable them to interact with other molecules existing in lipid rafts. Further studies will be necessary to clarify the detailed mechanism of $P2Y_2$ receptor localization within lipid rafts

In the present study, we have shown that $P2Y_2$ receptor-mediated activation of the $G_{q/11}$-PLC-Ca^{2+} pathway in lipid rafts enables effective cell migration. The $P2Y_2$ receptor is known to work as a sensor for cell migration (Elliott et al., 2009) and has an important role in physiological and pathological processes like brain injury (Norton et al., 1992). Analysis of the spatiotemporal regulation mechanism will be helpful to understand the physiological and pathological processes in future.

Acknowledgments

We are grateful to Dr. Haruhiro Higashida (Kanazawa University, Kanazawa, Japan) and Dr. Hitoshi Kurose (Kyushu University, Fukuoka, Japan) for the generous gifts of NG108-15 cells and adenovirus encoding p115-RGS, respectively. We are also grateful to Astellas Pharma Inc. (Tokyo, Japan) for providing YM254890. We are further grateful to Dr. Isao Matsuoka (Takasaki University of Health and Welfare, Takasaki, Japan) for his personal communications on lipid rafts.

References

Booden MA, Siderovski DP and Der CJ (2002) Leukemia-associated Rho guanine nucleotide exchange factor promotes Gαq-coupled activation of RhoA. *Mol Cell Biol* **22**:4053-4061.

Brown DA and London E (2000) Structure and function of sphingolipid- and cholesterol-rich membrane rafts. *J Biol Chem* **275**:17221-17224.

Edwards DC, Sanders LC, Bokoch GM and Gill GN (1999) Activation of LIM-kinase by Pak1 couples Rac/Cdc42 GTPase signalling to actin cytoskeletal dynamics. *Nat Cell Biol* **1**:253-259.

Elliott MR, Chekeni FB, Trampont PC, Lazarowski ER, Kadl A, Walk SF, Park D, Woodson RI, Ostankovich M, Sharma P, Lysiak JJ, Harden TK, Leitinger N and Ravichandran KS (2009) Nucleotides released by apoptotic cells act as a find-me signal to promote phagocytic clearance. *Nature* **461**:282-286.

Erb L, Liu J, Ockerhausen J, Kong Q, Garrad RC, Griffin K, Neal C, Krugh B, Santiago-Perez LI, Gonzalez FA, Gresham HD, Turner JT and Weisman GA (2001) An RGD sequence in the $P2Y_2$ receptor interacts with $\alpha_V\beta_3$ integrins and is required for G_o-mediated signal transduction. *J Cell Biol* **153**:491-501.

Foster LJ, De Hoog CL and Mann M (2003) Unbiased quantitative proteomics of lipid rafts reveals high specificity for signaling factors. *Proc Natl Acad Sci U S A* **100**:5813-5818.

Greig AV, Linge C, Cambrey A and Burnstock G (2003) Purinergic receptors are part of

a signaling system for keratinocyte proliferation, differentiation, and apoptosis in human fetal epidermis. *J Invest Dermatol* **121**:1145-1149.

Honma S, Saika M, Ohkubo S, Kurose H and Nakahata N (2006) Thromboxane A_2 receptor-mediated $G_{12/13}$-dependent glial morphological change. *Eur J Pharmacol* **545**:100-108.

Iwabuchi K, Handa K and Hakomori S (1998) Separation of "glycosphingolipid signaling domain" from caveolin-containing membrane fraction in mouse melanoma B16 cells and its role in cell adhesion coupled with signaling. *J Biol Chem* **273**:33766-33773.

Keller P and Simons K (1998) Cholesterol is required for surface transport of influenza virus hemagglutinin. *J. Cell Biol.* **140**:1357-1367.

Kohno T, Wada A and Igarashi Y (2002) N-glycans of sphingosine 1-phosphate receptor Edg-1 regulate ligand-induced receptor internalization. *FASEB J.* **16**:983-992.

Liao Z, Seye CI, Weisman GA and Erb L (2007) The $P2Y_2$ nucleotide receptor requires interaction with αv integrins to access and activate G_{12}. *J Cell Sci* **120**:1654-1662.

Liu J, Liao Z, Camden J, Griffin KD, Garrad RC, Santiago-Perez LI, Gonzalez FA, Seye CI, Weisman GA and Erb L (2004) Src homology 3 binding sites in the $P2Y_2$ nucleotide receptor interact with Src and regulate activities of Src, proline-rich tyrosine kinase 2, and growth factor receptors. *J. Biol. Chem.* **279**:8212-8218.

Lustig KD, Shiau AK, Brake AJ and Julius D (1993) Expression cloning of an ATP

receptor from mouse neuroblastoma cells. *Proc Natl Acad Sci U S A* **90**:5113-5117.

Lutz S, Shankaranarayanan A, Coco C, Ridilla M, Nance MR, Vettel C, Baltus D, Evelyn CR, Neubig RR, Wieland T and Tesmer JJ (2007) Structure of $G\alpha_q$-p63RhoGEF-RhoA complex reveals a pathway for the activation of RhoA by GPCRs. *Science* **318**:1923-1927.

Matsuoka I, Zhou Q, Ishimoto H and Nakanishi H (1995) Extracellular ATP stimulates adenylyl cyclase and phospholipase C through distinct purinoceptors in NG108-15 cells. *Mol Pharmacol* **47**:855-862.

Moore GA, McConkey DJ, Kass GE, O'Brien PJ and Orrenius S (1987) 2,5-Di(tert-butyl)-1,4-benzohydroquinone--a novel inhibitor of liver microsomal Ca^{2+} sequestration. *FEBS Lett* **224**:331-336.

Morris AJ and Malbon CC (1999) Physiological regulation of G-protein linked signaling. *Physiol. Rev.* **79**:1373-1430.

Nakahata N, Abe MT, Matsuoka I and Nakanishi H (1990) Mastoparan inhibits phosphoinositide hydrolysis via pertussis toxin-insensitive G-protein in human astrocytoma cells. *FEBS Lett* **260**:91-94.

Neumann-Giesen C, Falkenbach B, Beicht P, Claasen S, Luers G, Stuemer CA, Herzog V and Tikkanen R (2004) Membrane and raft association of reggie-1/flotillin-2: role of myristoylation, palmitoylation and oligomerization and induction of filopodia by overexpression. *Biochem. J.* **378**:509-518.

North RA (2002) Molecular physiology of P2X receptors. *Physiol. Rev.* **82**:1013-1067.

Norton WT, Aquino DA, Hozumi I, Chiu FC and Brosnan CF (1992) Quantitative aspects of reactive gliosis: a review. *Neurochem Res* **17**:877-885.

Oh P and Schnitzer JE (2001) Segregation of heterotrimeric G proteins in cell surface microdomains. G_q binds caveolin to concentrate in caveolae, whereas G_i and G_s target lipid rafts by default. *Mol Biol Cell* **12**:685-698.

Ohashi K, Nagata K, Maekawa M, Ishizaki T, Narumiya S and Mizuno K (2000) Rho-associated kinase ROCK activates LIM-kinase 1 by phosphorylation at threonine 508 within the activation loop. *J Biol Chem* **275**:3577-3582.

Pike LJ and Miller JM (1998) Cholesterol depletion delocalizes phosphatidylinositol bisphosphate and inhibits hormone-stimulated phosphatidylinositol turnover. *J Biol Chem* **273**:22298-22304.

Ralevic V and Burnstock G (1998) Receptors for purines and pyrimidines. *Pharmacol. Rev.* **50**:413-492.

Rojas RJ, Yohe ME, Gershburg S, Kawano T, Kozasa T and Sondek J (2007) $G\alpha_q$ directly activates p63RhoGEF and Trio via a conserved extension of the Dbl homology-associated pleckstrin homology domain. *J Biol Chem* **282**:29201-29210.

Rybin VO, Xu X, Lisanti MP and Steinberg SF (2000) Differential targetting of β–adrenergic receptor subtypes and adenylyl cyclase to cardiomyocyte caveolae: A mechanism to functionally regulate the cAMP signaling pathway. *J. Biol. Chem.* **275**:41447-41457.

Sak K and Webb TE (2002) A retrospective of recombinant P2Y receptor subtypes and

their pharmacology. *Arch. Biochem. Biophys.* **397**:131-136.

Schlegel A, Pestell RG and Lisanti MP (2000) Caveolins in cholesterol trafficking and signal transduction: implications for human disease. *Front Biosci.* **5**:D929-D937.

Simons K and Ikonen E (1997) Functional rafts in cell membranes. *Nature* **387**:569-572.

Sugama J, Ohkubo S, Atsumi M and Nakahata N (2005) Mastoparan changes the cellular localization of $G\alpha_{q/11}$ and Gβ through its binding to ganglioside in lipid rafts. *Mol Pharmacol* **68**:1466-1474.

Takasaki J, Saito T, Taniguchi M, Kawasaki T, Moritani Y, Hayashi K and Kobori M (2004) A novel $G\alpha_{q/11}$-selective inhibitor. *J Biol Chem* **279**: 47438-47445.

Toselli M, Taglietti V, Parente V, Flati S, Pavan A, Guzzi F and Parenti M (2001) Attenuation of G protein-mediated inhibition of N-type calcium currents by expression of caveolins in mammalian NG108-15 cells. *J. Physiol.* **536**:361-373.

Vainio S, Heino S, Mansson J, P. F, Kuismanen E, Vaarala O and Ikonen E (2002) Dynamic association of human insulin receptor with lipid rafts in cells lacking caveolae. *EMBO reports* **3**:95-100.

Varma R and Mayor S (1998) GPI-anchored proteins are organized in submicron domains at the cell surface. *Nature* **394**:798-801.

Wang M, Kong Q, Gonzalez FA, Sun G, Erb L, Seye C and Weisman GA (2005) P2Y nucleotide receptor interaction with α integrin mediates astrocyte migration. *J Neurochem* **95**:630-640.

Watano T, Matsuoka I, Ogawa K and Kimura J (2002) Effects of anions on

ATP-induced $[Ca^{2+}]_i$ increase in NG108-15 cells. *Jpn J Pharmacol* **89**:302-308.

Xu J, Wang F, Van Keymeulen A, Herzmark P, Straight A, Kelly K, Takuwa Y, sugimoto N, Mitchinson T and Bourne HR (2003) Divergent signals and cytoskeletal assemblies regulate self-organizing polarity in neutrophils. *Cell* **114**:201-214.

Zidovetzki R and Levitan I (2007) Use of cyclodextrins to manipulate plasma membrane cholesterol content: evidence, misconceptions and control strategies. *Biochim Biophys Acta* **1768**:1311-1324.

Footnotes

This work was supported in part by a Grant-in-Aid for Scientific Research from the Ministry of Education, Culture, Science, Sports and Technology of Japan [Grant 13771369] (to S.O.); and [Grants 14370737, 18058002, 19659011 and 20054002] (to N.N.); and a Grant-in-Aid from the Mitsubishi Foundation (to N.N.).

JPET Fast Forward. Published on May 28, 2010 as DOI: 10.1124/jpet.110.167528
This article has not been copyedited and formatted. The final version may differ from this version.

Legends for Figures

Fig. 1. Effect of methyl-β-cyclodextrin (CD) on cholesterol extraction and lactate dehydrogenase (LDH) release from NG108-15 cells. (A) Extraction of cholesterol from membranes by CD-treatment. Suspended cells were treated with indicated concentrations of CD for 30 min at 37°C. The cholesterol level in the incubation medium (●) or in the cells (○) was determined. Each point represents the mean ± SEM of three determinations, and data are representative of two independent experiments. Significant difference compared to the value without CD treatment (*p < 0.05; **p < 0.01). (B) Effect of CD on LDH release. NG108-15 cells in the 12-well plates were treated with the indicated concentrations of CD for 30 min at 37°C. The LDH activity released into the medium was expressed as % of total cellular LDH activity. Each point represents the mean ± SEM of three determinations, and data are representative of two independent experiments.

Fig. 2. Characterization of isolated lipid raft fractions by sucrose-density gradient centrifugation. NG108-15 cells pretreated with (●) or without 10 mM CD (○) for 30 min at 37°C were lysed by the lysis buffer, and cell lysate were fractionated by a sucrose-density gradient. Cholesterol content (A) in each fraction separated by sucrose-density gradient was determined as described in "Materials and methods", and data are representative of three independent experiments. NG 108-15 cells pretreated with or without 10 mM CD for 30 min at 37°C were lysed, and cell lysates were

JPET Fast Forward. Published on May 28, 2010 as DOI: 10.1124/jpet.110.167528
This article has not been copyedited and formatted. The final version may differ from this version.

fractionated by sucrose-density gradient centrifugation. Distribution of flotillin-1 (B), Ganglioside GM1 (C), $G\alpha_{q/11}$ (D) and $P2Y_2$ receptor (E) were determined. Equal volumes derived from each sample were analyzed by dot blotting (C) or Western blotting (B, D, E). CD-treated or non-treated cell lysates before separation by sucrose gradient centrifugation (lys) were also analyzed as a positive control. Representative results are shown from three independent experiments.

Fig. 3. Inhibitory effect of CD on UTP-induced cell migration. (A) Effect of CD on cell viability. NG 108-15 cells were treated with CD at the indicated concentrations. Cells treated with CD for 30 min were further incubated for 18 hr after replacing medium with serum-free medium without CD. Cells treated with CD for 18 hr were incubated for 18 hr without the replacement of medium and cell viability was measured using the MTT assay. Cell viability was expressed as a percentage of the control. Each point represents the mean ± SEM of three determinations. (B) Time course of cholesterol content in the plasma membrane after CD treatment. NG 108-15 cells grown in 6-well plates were treated with 10 mM CD for 30 min at 37°C. Following CD treatment, medium was replaced with serum-free medium and cells were further incubated, as indicated time. Cholesterol level of plasma membranes was determined. Each column represents the mean ± S.E.M. of three experiments. * indicates a significant difference compared with non-treated CD cells (*$p < 0.05$). (C, D) Effect of CD on UTP-induced cell migration. After NG 108-15 cells were pretreated with or without 10 mM CD or vehicle for 30 min at 37°C, they were collected and incubated in

JPET Fast Forward. Published on May 28, 2010 as DOI: 10.1124/jpet.110.167528
This article has not been copyedited and formatted. The final version may differ from this version.

the upper chamber in the presence or absence of 100 μM UTP in the lower chamber. After 18 hr, cells migrating to the lower side of the membrane were visualized by staining with Hoechst 33258 (C) and the number of migrating cells was counted (D). Each column represents the mean ± S.E.M. of nine experiments. * indicates a significant difference compared with the value of control or UTP treated cells (*p < 0.01).

Fig. 4. Involvement of $G_{q/11}$ in UTP-induced cell migration. (A) Concentration-dependent effect of CD on the UTP-induced phosphoinositide hydrolysis. [^{3}H]-Inositol-prelabeled NG 108-15 cells were incubated with the indicated concentrations of CD for 30 min at 37°C. After washing, cells were stimulated with (●) or without (○) 100 μM UTP in the presence of 10 mM LiCl for 10 min at 37°C. Each point represents the mean ± SEM of three determinations. * indicates a significant difference compared with values without CD treatment (*p < 0.05). (B) Effect of CD on $[Ca^{2+}]_i$ elevation. Cells were pretreated with or without 10 mM CD for 30 min at 37°C, and were loaded with 1 μM Fura-2/AM for 15 min at 37°C. After washing, cells were stimulated with ATP, UTP, BzATP (each 100 μM) or tBuBHQ (10 μM). (C) The summarized results of $[Ca^{2+}]_i$ elevation in the cells pretreated with (hatched column) or without CD (open column). Each column represents the mean ± SEM of four experiments. * indicates a significant difference compared to the value without CD treatment (*p < 0.05). (D) Effect of YM254890 on UTP-induced cell migration. NG108-15 cells pretreated with or without 1 μM YM254890for 30 min at

37°C were collected and incubated in the upper chamber in the presence or absence of 100 μM UTP in the lower chamber. After 18 hr, the number of cells migrating to the lower side of the membrane was counted. Each column represents the mean ± SEM of nine experiments. * indicates a significant difference compared with control or UTP values (*$p < 0.05$).

Fig. 5. Effect of CD-exogenous cholesterol complex on cellular cholesterol level, UTP-induced phosphoinositide hydrolysis and cell migration. (A) Cellular cholesterol contents after CD-cholesterol complex treatment. NG 108-15 cells were seeded on 6 well plate (2 x 10^5 cells) and incubated for 48 hr. After 48 hr, the cells were treated with or without 10 mM CD containing various concentrations of cholesterol for 30 min at 37°C. Then, the cholesterol contents in the whole cells were determined. The first column labeled with "no CD" indicates the result in the absence of CD. Each column represents the mean ± SEM of three determinations. * indicates a significant difference compared to the value without CD treatment (*$p < 0.05$). (B) Effect of CD-cholesterol complex on UTP-induced phosphoinositide hydrolysis. [^{3}H]-Inositol-prelabeled NG 108-15 cells were treated with or without 10 mM CD containing various concentrations of cholesterol for 30 min at 37°C. After washing, cells were stimulated with 100 μM UTP in the presence of 10 mM LiCl for 10 min at 37°C. The first and second columns labeled with "no CD" indicate the result in the absence of CD. Each column represents the mean ± SEM of three determinations. * indicates a significant difference compared with values without CD treatment (*$p <$

JPET Fast Forward. Published on May 28, 2010 as DOI: 10.1124/jpet.110.167528
This article has not been copyedited and formatted. The final version may differ from this version.

0.05). (C) Effect of CD-cholesterol complex on UTP-induced cell migration. After NG 108-15 cells were pretreated with or without 75% saturated 10 mM CD-cholesterol complex for 30 min at 37°C, they were collected and incubated in the upper chamber in the presence or absence of 100 μM UTP in the lower chamber. After 18 hr, the number of migrating cells was counted. The first and second columns labeled with "no CD" indicate the result in the absence of CD. Each column represents the mean ± S.E.M. of three experiments. * indicates a significant difference compared with the value of UTP-treated cells (*$p < 0.05$). (D) Effect of CD on $[Ca^{2+}]_i$ elevation after 18 hr. NG 108-15 cells were pretreated with or without 10 mM CD for 30 min at 37°C. Then medium was washed out and the cells were incubated for additional 18 hr. After 18 hr, the cells were loaded with 1 μM Fura-2/AM for 15 min at 37°C. After washing, the cells were stimulated with 100 μM UTP. Each column represents the mean ± S.E.M. of four experiments. * indicates a significant difference compared with the value of UTP-treated cells (*$p < 0.05$).

Fig. 6. $G_{q/11}$-dependent Rho-A activation. (A) $G_{q/11}$-dependent Rho-A activation. Cells pretreated with or without 10 mM CD, 1 μM YM254890 or 5 μg/ml anti-integrin α_v antibody for 30 min were stimulated with 100 μM UTP for 3 min. Rho-A activity was analyzed after UTP stimulation as described in Materials and Methods. (B) Quantitative analysis of Rho-A activation. The density of GTP-Rho-A was normalized with corresponding that of total Rho-A, then the normalized amounts of GTP-Rho-A were shown as % of UTP stimulation. Each column represents the mean ± S.E.M. of

JPET Fast Forward. Published on May 28, 2010 as DOI: 10.1124/jpet.110.167528
This article has not been copyedited and formatted. The final version may differ from this version.

three experiments. * indicates a significant difference compared with the value of UTP treated cells (*$p < 0.05$).

Fig. 7. $G_{q/11}$-dependent stress fiber formation. $G_{q/11}$-dependent stress fiber formation. NG 108-15 cells were pretreated with 10 mM CD for 30 min, 1 μM YM254890 for 15 min or 5 μg/ml PTX for 24 hr were stimulated with 100 μM UTP for 30 min. Stress fibers were visualized by staining F-actin with Rhodamine-Phalloidin. Representative images are shown for three experiments (A-E). The population of cells forming stress fiber was quantitated (F). Each column represents the mean ± S.E.M. of three experiments. * indicates a significant difference compared with the value of UTP treated cells (*$p < 0.05$).

Fig. 8. $G_{q/11}$-dependent phosphorylation of cofilin. (A) $G_{q/11}$-dependent phosphorylation of cofilin. NG 108-15 cells pretreated with or without 1 μM YM254890 for 30 min, 5 μg/ml PTX for 24 hr or vehicle were stimulated with 100 μM UTP for 3 min. (B) Summarized data of $G_{q/11}$-dependent phosphorylation of cofilin. (C) Lipid raft- and integrin α_v-dependent phosphorylation of cofilin. NG 108-15 cells pretreated with or without 10 mM CD or 5 μg/ml anti-integrin α_v antibody for 30 min were stimulated with 100 μM UTP for 3 min. (D) Summarized data of $G_{q/11}$-dependent phosphorylation of cofilin. (E) $G_{q/11}$-independent phosphorylation of cofilin by LPA. NG 108-15 cells pretreated with or without 1 μM YM254890 for 30 min were stimulated with 10 μM LPA for 3 min. (F) Summarized data of $G_{q/11}$-independent

phosphorylation of cofilin by LPA. (G) $G_{12/13}$-independent phosphorylation of cofilin. NG 108-15 cells were infected with recombinant adenoviruses encoding control (vector-GFP) or p115-RGS at MOI of 100 or 150 for 48 hr. Then, cells were stimulated with 100 μM UTP or 10 μM LPA for 3 min after 8 hr starvation. (H) Summarized data of the effect of p115-RGS at MOI of 150 on UTP-induced phosphorylation of cofilin. (I) Summarized data of the effect of p115-RGS at MOI of 150 on LPA-induced phosphorylation of cofilin. (J) ROCK-dependent phosphorylation of cofilin. NG 108-15 cells pretreated with or without 1 μM Y27632 (Y) for 15 min were stimulated with 100 μM UTP for 3 min. (K) Summarized data of ROCK-dependent phosphorylation of cofilin. Phospho-cofilin (p-cofilin) was determined by immunoblotting with anti-phospho cofilin antibody. β-tubulin was used as an internal control (A, C, E, G and J). Phosphorylation of cofilin was normalized with the corresponding β-tubulin then normalized amounts of phosphorylation of cofilin were shown as % of UTP stimulation (B, D, H and K) or LPA stimulation (F, I). Each column of the summarized data represents the mean ± S.E.M. of three experiments (B, D, F, I, H and K). * indicates a significant difference compared with the value of UTP- or LPA-treated cells (*$p < 0.05$).

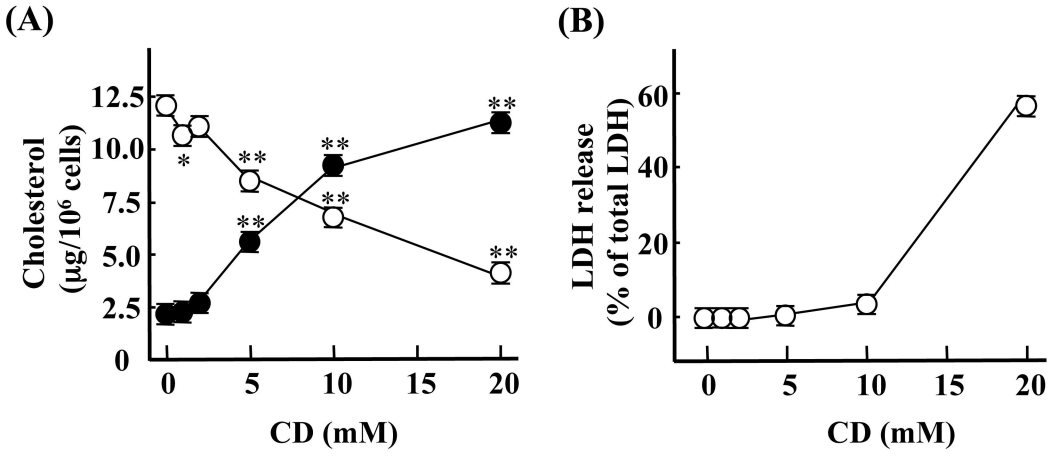
(A)
Cholesterol (μg/10⁶ cells)
12.5
10.0
7.5
5.0
2.5
0
0
5
10
15
20
CD (mM)
*
**
**
**
**
**
(B)
LDH release (% of total LDH)
60
40
20
0
0
5
10
15
20
CD (mM)

Fig. 1.

JPET Fast Forward. Published on May 28, 2010 as DOI: 10.1124/jpet.110.167528
This article has not been copyedited and formatted. The final version may differ from this version.

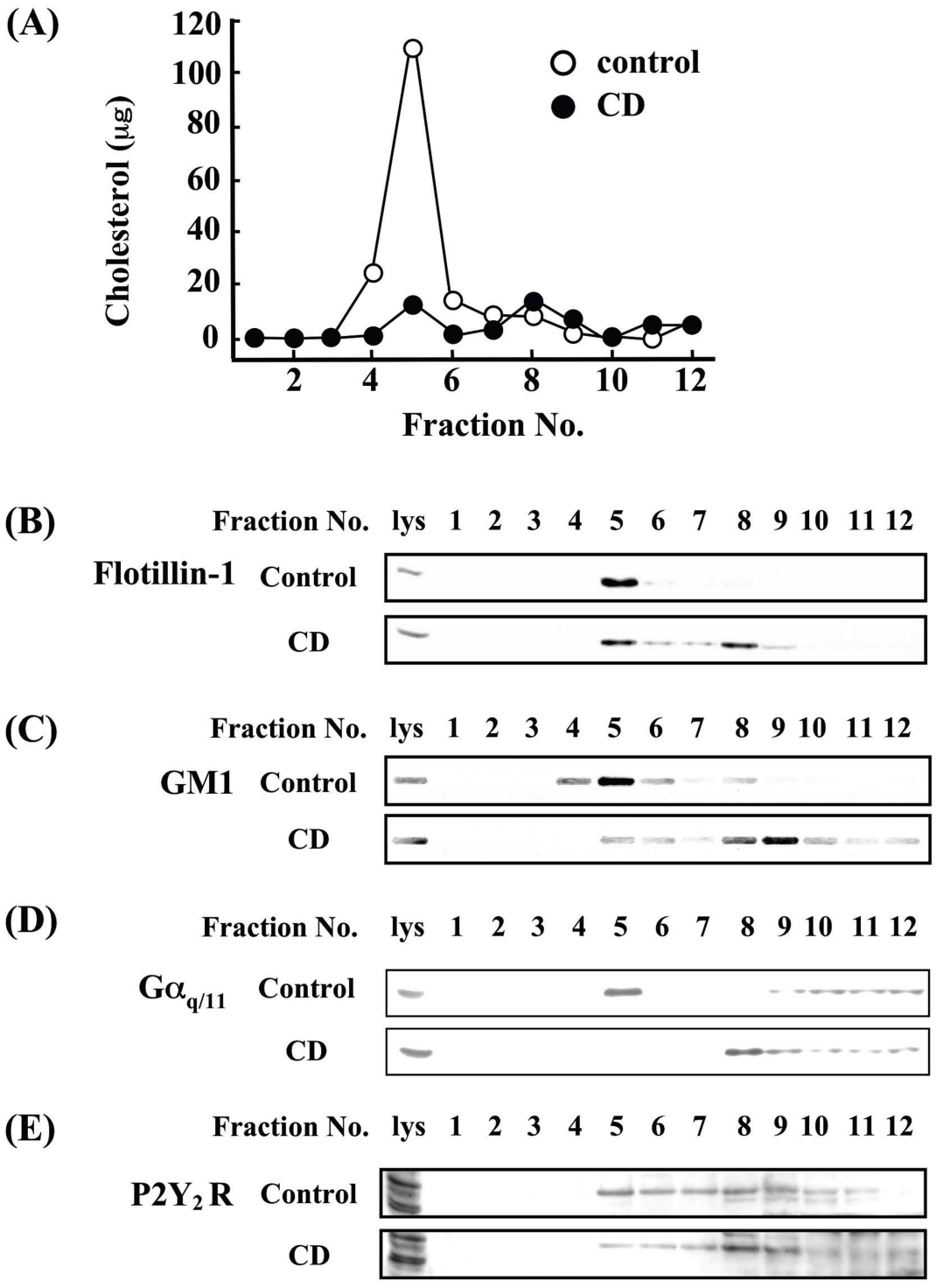

Fig. 2.

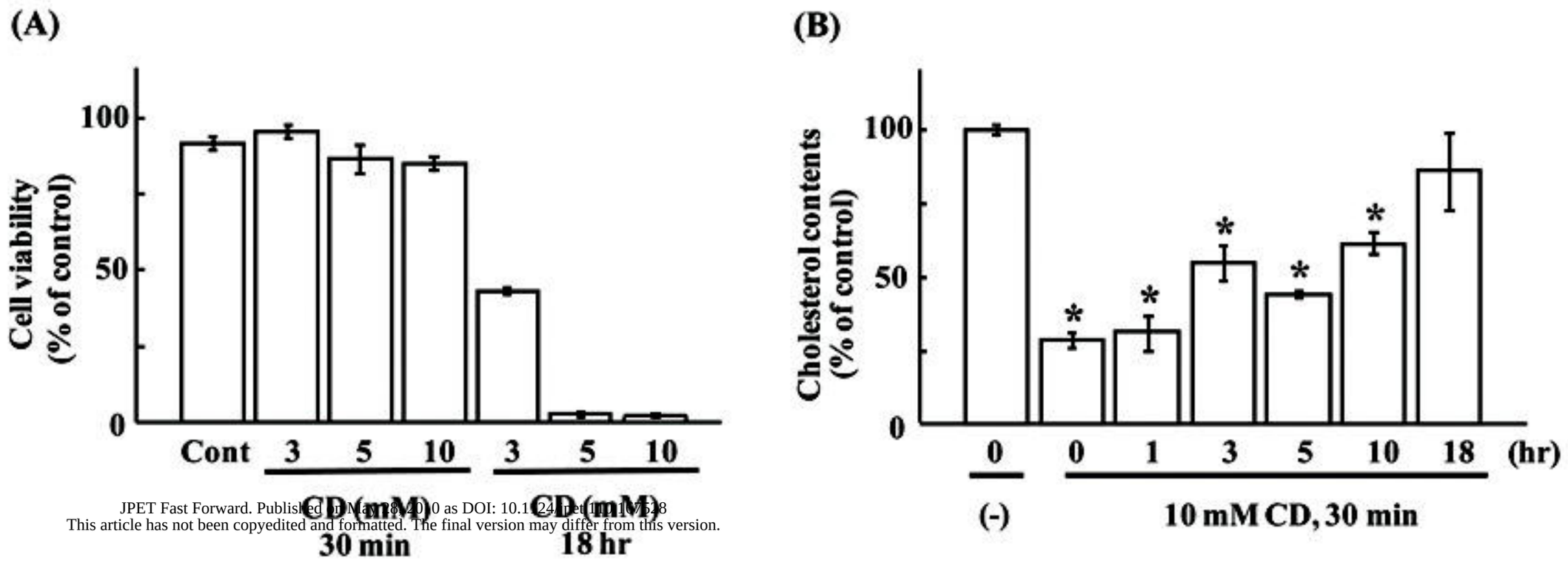

Fig. 3.

JPET Fast Forward. Published on May 28, 2010 as DOI: 10.1124/jpet.110.167528

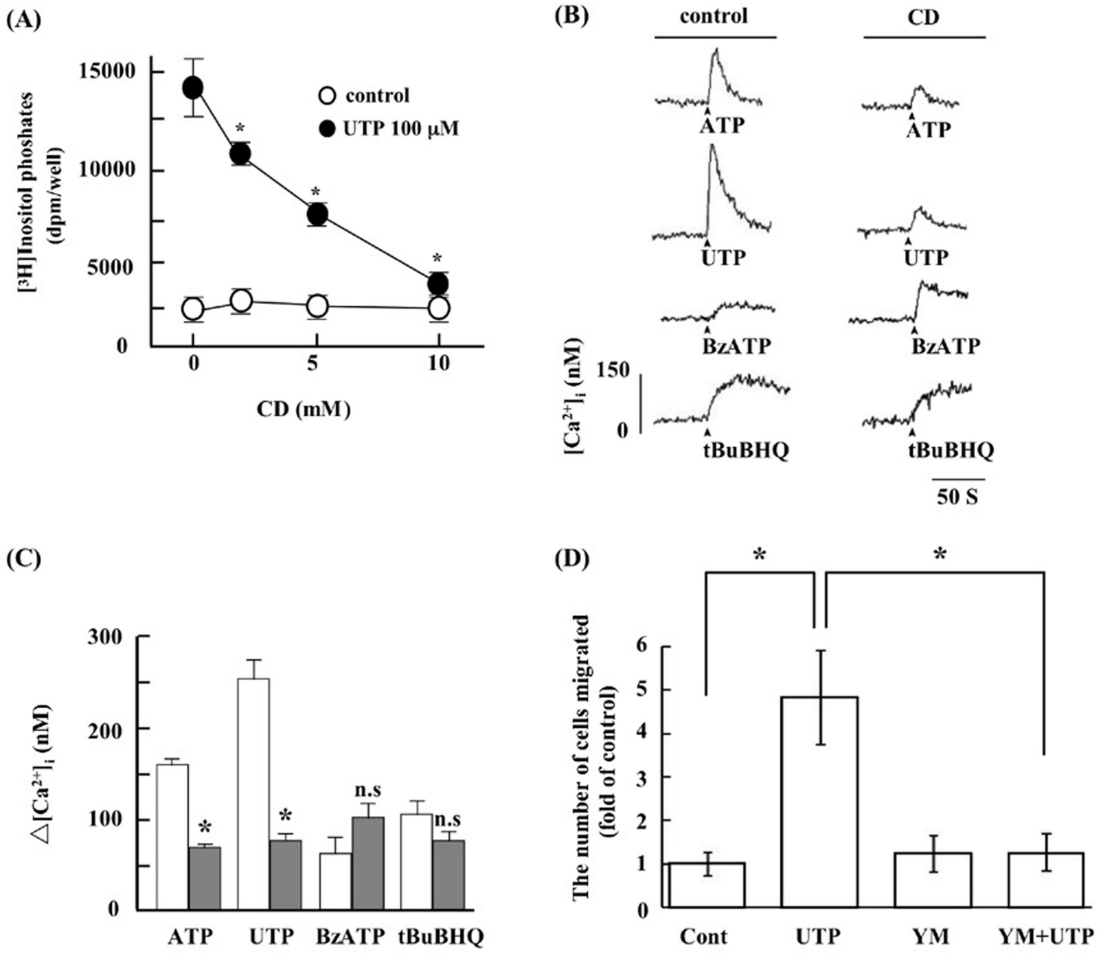

Fig. 4

JPET Fast Forward. Published on May 28, 2010 as DOI: 10.1124/jpet.110.167528
This article has not been copyedited and formatted. The final version may differ from this version.

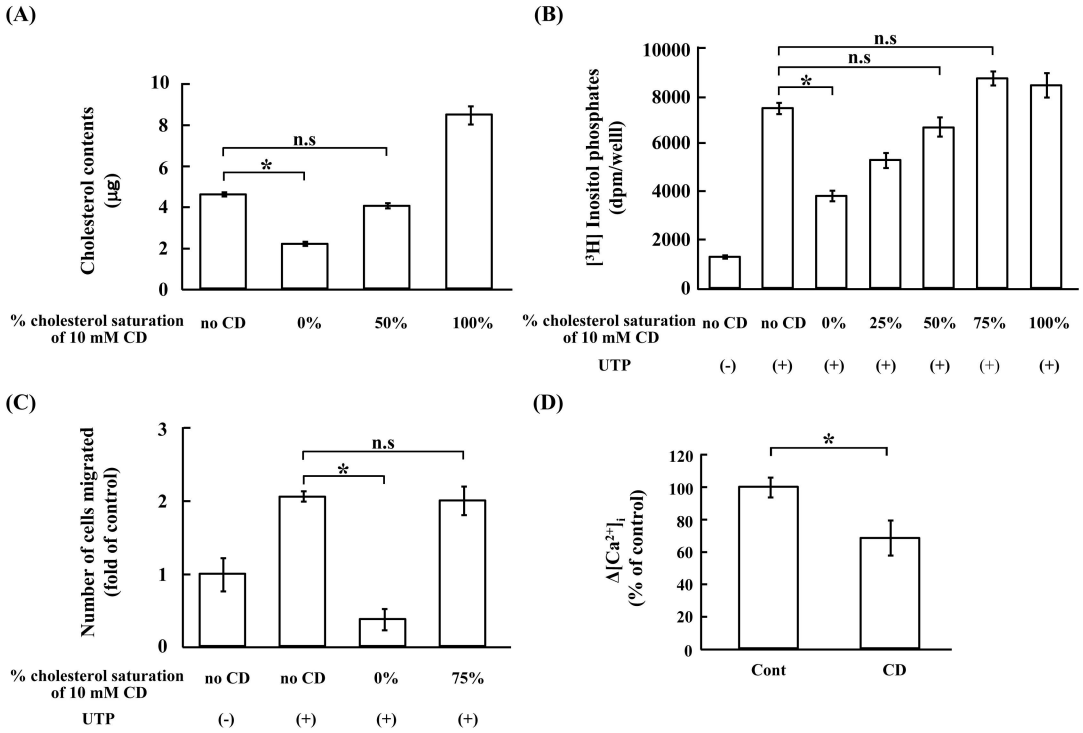

Fig. 5.

JPET Fast Forward. Published on May 28, 2010 as DOI: 10.1124/jpet.110.167528

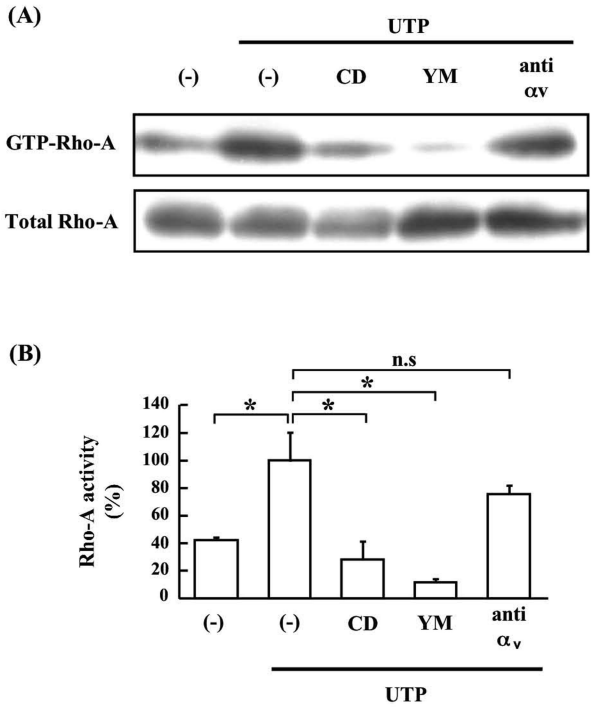

Fig. 6

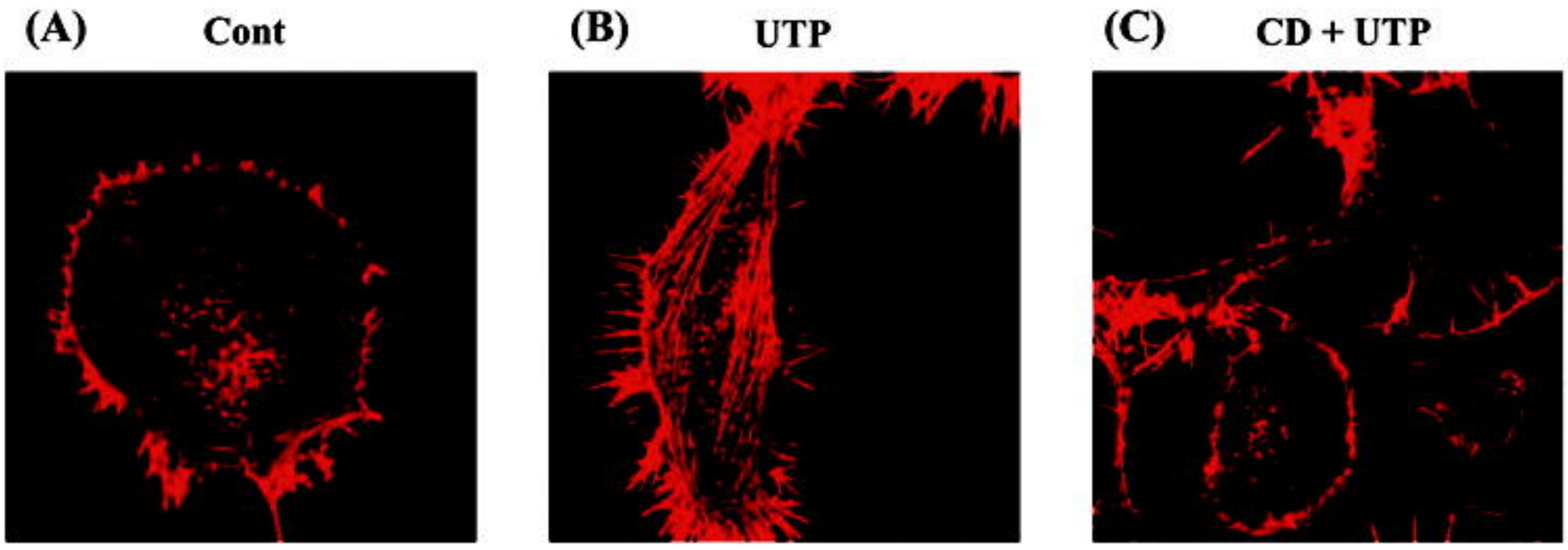

JPET Fast Forward. Published on May 28, 2010 as DOI: 10.1124/jpet.110.167528
This article has not been copyedited and formatted. The final version may differ from this version.

Fig. 7.

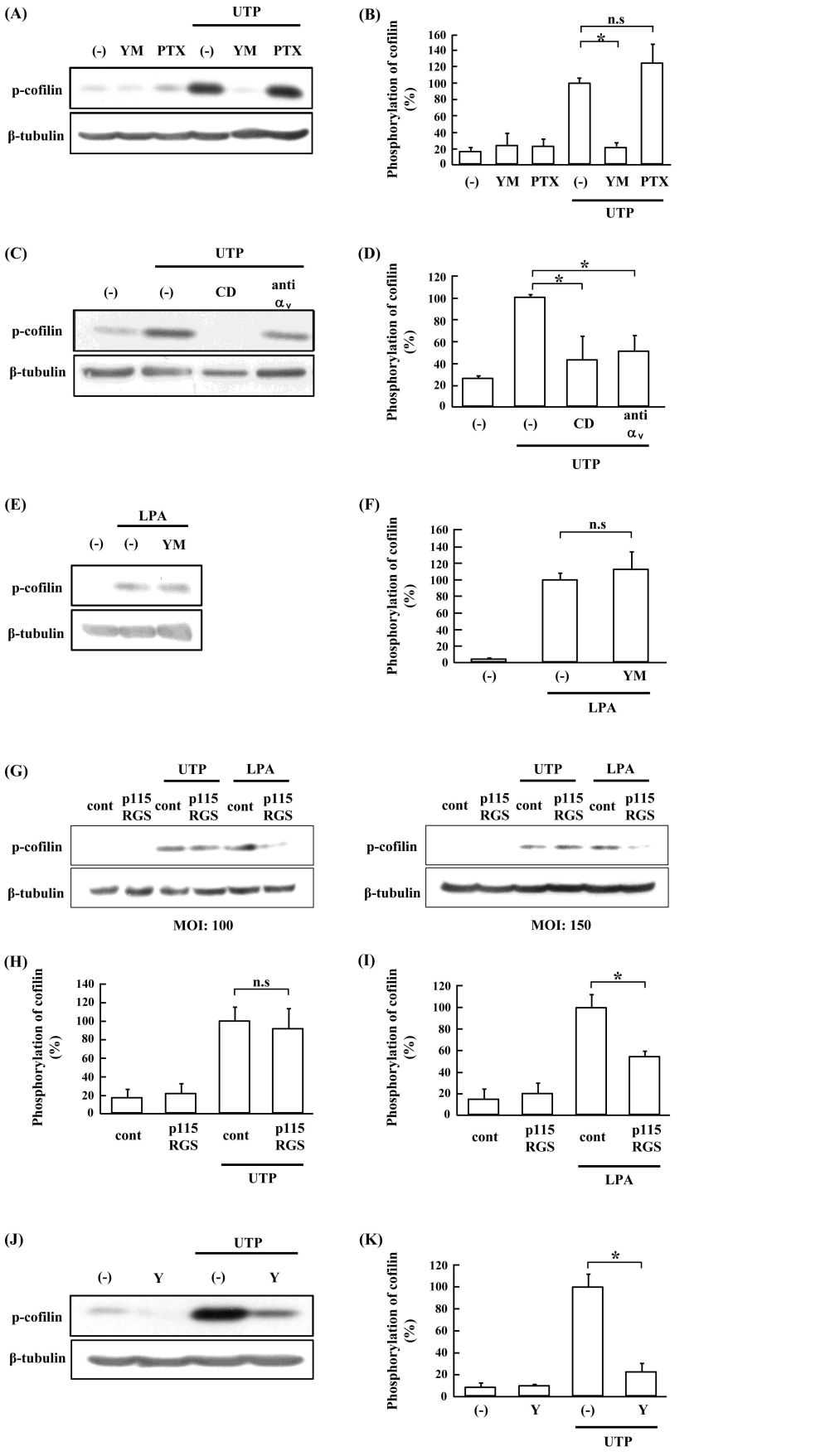
(A)
UTP
(-) YM PTX (-) YM PTX
p-cofilin
β-tubulin
(B)
Phosphorylation of cofilin (%)
n.s
*
(-) YM PTX (-) YM PTX
UTP
(C)
UTP
(-) (-) CD anti αv
p-cofilin
β-tubulin
(D)
Phosphorylation of cofilin (%)
*
*
(-) (-) CD anti αv
UTP
(E)
LPA
(-) (-) YM
p-cofilin
β-tubulin
(F)
Phosphorylation of cofilin (%)
n.s
(-) (-) YM
LPA
(G)
UTP LPA
cont p115 RGS cont p115 RGS cont p115 RGS
p-cofilin
β-tubulin
MOI: 100
MOI: 150
(H)
Phosphorylation of cofilin (%)
n.s
cont p115 RGS cont p115 RGS
UTP
(I)
Phosphorylation of cofilin (%)
*
cont p115 RGS cont p115 RGS
LPA
(J)
UTP
(-) Y (-) Y
p-cofilin
β-tubulin
(K)
Phosphorylation of cofilin (%)
*
(-) Y (-) Y
UTP

Fig. 8.